ELSEVIER

Nuclear Physics A 654 (1999) 579–596

NUCLEAR PHYSICS A

www.elsevier.nl/locate/npe

3.5-eV isomer of ^{229m}Th: How it can be produced

F.F. Karpeshin [a,b], I.M. Band [c], M.B. Trzhaskovskaya [c]

[a] *Departamento de Física, Universidade de Coimbra, P-3000 Coimbra, Portugal*

[b] *Institute of Physics, St. Petersburg University, RU-198904 St. Petersburg, Russia*

[c] *Petersburg Nuclear Physics Institute, RU-188350 Gatchina, Leningrad region, Russia*

Received 2 September 1998; revised 17 May 1999; accepted 18 May 1999

Abstract

Various schemes of producing the 3.5-eV isomer of ^{229m}Th by radiative pumping the atom of ^{229}Th in the ground state are considered. Due to the resonance properties of the electron shell, some of the schemes turn out to be more effective than radiative pumping the bare nucleus of the same element.

PACS: 20.00

1. Introduction

Study of the unique low-energy (3.5 ± 1.0) eV isomer of ^{229}Th [1,2] is of great interest from many viewpoints (see e.g. Refs. [3–14] and references cited therein). At the same time, for application of the 3.5-eV isomer of ^{229}Th one needs first of all much more precise knowledge of its properties, such as the separation energy of the doublet states, and the electromagnetic strength of the transition. Specifically, for many possible laser applications, the present corridor for the separation energy is too large in comparison with the line widths of modern lasers, which can be 1 Hz and even less.

Study of the properties of the isomer also requires practical methods of producing the source in enough quantities. In α decay of ^{233}U, the isomeric yield of Th nuclei is of the order of 10%. This way of getting the isomeric source has been used in experiments [11–14]. The isomeric nuclei, however, undergo the radiative transition to the ground state with a lifetime of 1 to 50 hours [5,6,10], which precludes collecting considerable amounts of the isomer.

A much more attractive way lies in the use of a pure ^{229}Th source. The lifetime of the ^{229}Th nuclei in the ground state is about 7000 years, which allows one to

0375-9474/99/$ - see front matter
PII S0375-9474(99)00303-6

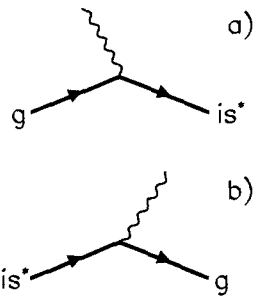

Fig. 1. (a) Feynman graph of photoexcitation of a nucleus. The double line specifies the nuclear transition from the ground (g) to the isomer (is*) state. (b) Feynman graph of the reverse process of deexcitation of the nucleus via radiative transition.

collect enough quantities of the nuclide. The isomeric state can be populated e.g. by resonance laser radiation [4,5,3,8,9]. In principle, this way even allows one to reach an inverse population of the levels [5]. It is, however, still important to clarify the role the electron shell plays in this method, as well as in other schemes proposed in the above references. On one hand, the shell screens the nucleus from the outer fields. But it can work as a resonator, if there is an electron transition with energy close to the nuclear one. Interplay of these two ways of things is studied in detail in Sections 2 and 3. For this purpose, various mechanisms of the nuclear excitation by resonance laser radiation have been considered in detail in Sections 2 and 3. Their cross-sections are calculated and compared to that for a bare nucleus. It is surprising to a certain extent that direct resonance pumping of the neutral atom turns out to be ineffective. Some more complicated schemes, however, hit the purpose. Corresponding cross-sections happen to be many times higher than that for a bare nucleus.

Magnetic interaction of the electrons with the nuclei can also be used for excitation of the isomeric state. Consider the collision of a one-electron atom in the $1s$ state with a lead target nucleus. The electron produces a tremendous magnetic field in the vicinity of the nucleus. Prompt removing of the electron in the collision induces a related change of the potential, giving rise to the shake effects in the system [16]. The effects can manifest themselves via excitation (shake-on) or disintegration of the system (shake-off). The probability of excitation of the 3.5-eV isomer brought about by sudden ionisation of the electron shell is considered in Section 4. This method is considered with respect to application to the muonic atoms. Results obtained are marvelous: the isomeric yield turns out to be practically 100%, that is an isomeric atom is obtained per every muon in the primary beam! The results obtained are summed up in Section 6.

2. Excitation by laser radiation

The Feynman graph of photoabsorption by a nucleus is given in Fig. 1a. The cross-section for photoexcitation of a single nuclear level is given by the following formula:

$$\sigma_\gamma(\omega) = 8\alpha\pi^3 \frac{L+1}{L} \frac{\omega^{2L-1}}{[(2L+1)!!]^2} B(\tau L; 0 \to \omega) \frac{\Gamma/2\pi}{\Delta^2 + (\Gamma/2)^2} \tag{1}$$

$$\equiv D_n(\omega) \frac{\Gamma/2\pi}{\Delta^2 + (\Gamma/2)^2} . \tag{2}$$

Here $\alpha = 1/137$ is the fine structure constant, τL is the type (electric, magnetic) and multipole order of the transition, $B(\tau L; 0 \to \omega)$ is the reduced probability of the radiative nuclear transition from the ground state to the excited one with the energy ω [1], and Γ is the total nuclear width. Through the detailed balancing principle, the reduced electromagnetic strength also determines the radiative width of the reverse nuclear transition from the excited to the ground state, $\Gamma_\gamma^{(n)}(\omega \to 0)$. It is didactic to perform further calculations in terms of the radiative width and internal conversion coefficients (ICC).

The expression for the radiative transition probability (Fig. 1b) reads as follows:

$$\Gamma_\gamma^{(n)}(\omega \to 0) = 8\alpha\pi \frac{L+1}{L} \frac{\omega^{2L+1}}{[(2L+1)!!]^2} B(\tau L; \omega \to 0) , \tag{3}$$

where

$$B(\tau L; \omega \to 0) = \frac{2I_0 + 1}{2I_\omega + 1} B(\tau L; 0 \to \omega) , \tag{4}$$

where I_0 and I_ω stand for the nuclear spins in the ground and excited states, respectively.

For simplicity, we suppose that the spectral width of the line of a laser is much greater than the width of the corresponding nuclear or atomic line. Taking into account Eqs. (3), (4), expression (1) for the absorption of the resonance radiation may then be presented in the following form:

$$\sigma_\gamma(\omega) = \Gamma_\gamma^{(n)}(\omega \to 0) \frac{2I_0 + 1}{2I_\omega + 1} \frac{\pi^2}{\omega^2} S(\omega) , \tag{5}$$

where $S(\omega)$ is the spectral density of the incident laser radiation.

Let the line width of the laser be $\Delta E \sim 10^{-5}$ eV, and the nuclear lifetime with respect to the radiative nuclear transition: $\lambda = 1/\Gamma_\gamma^{(n)} \approx 50$ hours. Then $S(\omega) \approx (\Delta E)^{-1} \sim 10^5$ eV^{-1}, and we arrive by means of Eq. (5) at the cross-section for pumping the isomer $\sigma_\gamma(\omega) \approx 170$ millibarn.

It is convenient to express $D(\omega)$ in terms of the radiative width of the reverse transition. Comparing Eqs. (5) and (2), we get

$$D_n(\omega) = \frac{\pi^2}{\omega^2} \Gamma_\gamma^{(n)}(\omega \to 0) \frac{2I_\omega + 1}{2I_0 + 1} . \tag{6}$$

In the presence of the electron shell, higher order resonance transitions involving the shell play an important role [17–20]. The basic idea in the present approach is to exploit a well-known process of NEET (Nuclear Excitation in Electron Transition) [21], and

[1] Relativistic units $\hbar = c = 1$ are used throughout the paper.

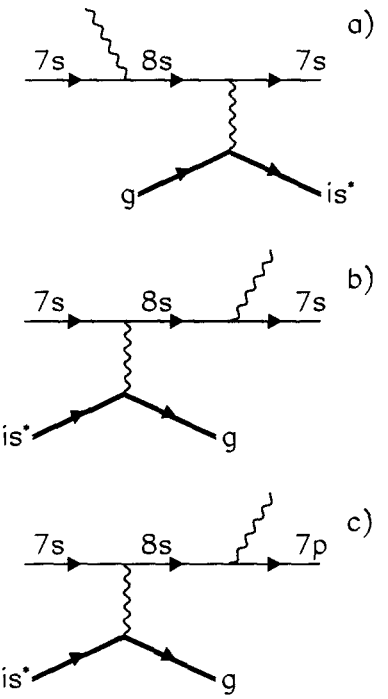

Fig. 2. Feynman graphs of the resonance nuclear excitation through the electron shell (a), of the reverse process of emission of a γ quantum by the nucleus (b), and that for the electron-bridge mechanism of nuclear deexcitation (c).

its reverse, which we call TEEN. NEET appears thus as a tool for transferring energy through the shell to the nucleus. Conversely, TEEN can be used as a trigger, for prompt release of the energy stored in nuclei [19,8]. It is essential that resonance properties of the electron shell are exploited in these processes. Effective resonance arises in the case of close frequencies of the nuclear and electron transitions. Such a situation is known in many nuclei: ^{197}Au, ^{179}Os, ^{237}Np, ^{235}U, and others (see e.g. Refs. [4–10] and references cited therein). Appropriate use of the resonance allows one to manipulate the rate of the nuclear processes [3]. Note that nonradiative transitions are also known in muonic atoms [15].

The simplest graph of nuclear photoabsorption via NEET is presented in Fig. 2a. The partial nuclear lifetime in the excited state (Fig. 2b) is also diminished due to the TEEN process. It essentially differs from the well-known mechanism of the electron bridge given in Fig. 2c. In the latter case, the transition would be much stronger because of the electric dipole vertex corresponding to the radiative deexcitation $8s$–$7p$.

The expression corresponding to the radiative width of Fig. 2b can be given as follows:

$$\Gamma_\gamma^{(2b)} = \frac{\alpha_d \Gamma_\gamma^{(a)}/2\pi}{\Delta^2 + (\Gamma^{(a)}/2)^2}\, \Gamma_\gamma^{(n)}(\omega \to 0)\,. \tag{7}$$

In Eq. (7) we introduced a notation $\Gamma_\gamma^{(a)}$ and $\Gamma^{(a)}$ for the radiative and total atomic

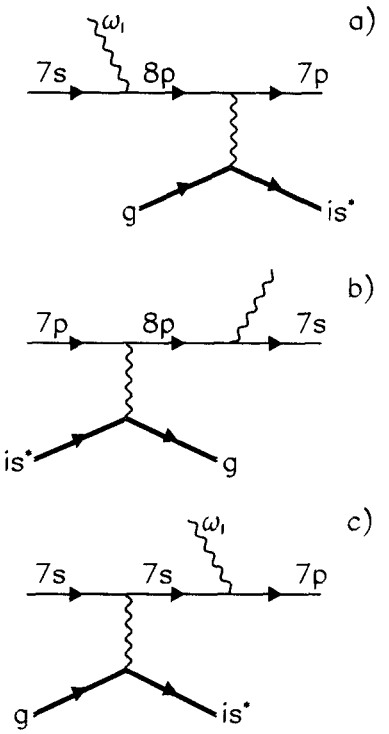

Fig. 3. Feynman graphs of nuclear excitation through the electron shell with the electric dipole vertex of interaction with the externally applied laser field (a), of the reverse process of nuclear deexcitation (b), and another mechanism of nuclear excitation with a different order of interaction of the electron shell with the nucleus and the electromagnetic field (c).

widths, respectively. α_d is a dimensional analogue of internal conversion coefficient (ICC). It is defined by means of the same formulae as usual ICC, but has dimension of energy [3].

Now the expression for the cross-section corresponding to the graph of Fig. 2a can be obtained by mere substitution of expression (7) for $\Gamma_\gamma^{(2b)}$ into Eq. (3) instead of $\Gamma_\gamma^{(n)}$. Then one arrives at the following expression for the ratio of the photoexcitation cross-sections through the electron shell to that for the bare nucleus:

$$R^{(2a)} = \frac{\alpha_d \Gamma_\gamma^{(a)}(8s \to 7s; \omega_n)/2\pi}{\Delta^2 + (\Gamma^{(a)}/2)^2}, \tag{8}$$

where $\Gamma_\gamma^{(a)}(np \to 7s; \omega_n)$ is the partial radiative width of the $np \to 7s$ transition, calculated at the energy ω_n.

One can try to further enhance the amplitude of Fig. 2a by replacing the M1 atomic radiative vertex with the much stronger electric dipole vertex. Thus we come to the graph of Fig. 3a for the nuclear excitation, and Fig. 3b for the radiative width of the related reverse process. The latter transition in fact occurs in the atom with the excited electron shell in the $7p$ state. The energy of the absorbed laser photon ω_l is equal to

the nuclear energy plus the excitation energy of the atom in the final state, that is $7p$–$7s$ transition:

$$\omega_l = \omega_n + \omega_{7p-7s}\,.$$

The corresponding cross-section and radiative probabilities can be calculated by means of the above formulae, replacing $7s$ and $8s$ states by the $7p$ and $8p$ ones, respectively. Explicitly, we arrive at the cross-section ratio R expressed as follows:

$$R^{(3a)} = \frac{\alpha_d(7p \to 8p)\,\Gamma_\gamma^{(a)}(8p \to 7s;\omega_l)}{2\pi[(\omega_n - \omega_{8p-7p})^2 + (\Gamma^{(a)}/2)^2]}\,. \tag{9}$$

A much stronger contribution comes in this case from a diagram of Fig. 3c, where interaction of the shell with the laser field and the nucleus is performed in the reverse order. After transferring energy ω_n to the nucleus, the electron goes to an intermediate state with an energy which is thus always below the real level. In this respect, strictly speaking, the electron shell is not put into a resonating state. The resonance condition is only fulfilled for the energy of the final electron state.

A strong enhancement, however, arises from the fact that the conversion transition occurs between the s states ($7s$–$7s$). In this case, as one can see from Table 1, the corresponding α_d values are by about three orders of magnitude higher than for a transition between p states, such as $7p$–$7p$ etc. This is due to the very small probability of the localisation of the $7p$ electron near the nucleus, as its wavefunction is zero at the origin [7]. The conversion factor R is given by the same formula (9), with the above modification of the energy of the intermediate state and conversion coefficient α_d:

$$R^{(3c)} = \frac{\alpha_d(7s \to 7s)\,\Gamma_\gamma^{(a)}(7p \to 7s;\omega_l)}{2\pi[(\omega_n + \omega_a)^2 + (\Gamma^{(a)}/2)^2]}\,, \tag{10}$$

where ω_a is the energy of the intermediate electron state in Fig. 3c, if different from the $7s$ state.

Another way of the nuclear excitation based on the two-photon radiative mechanism is shown in Fig. 4. There is no resonance restriction on the energy of the incoming photon in this amplitude, which would require knowing the nuclear energy, at present not available. The outgoing photon carries away excessive energy brought by the laser photon. The corresponding additional electromagnetic vertex thus arises as a necessary price one has to pay for fulfilling conservation of energy.

To calculate this diagram, let us consider the more detailed graph of Fig. 4b, where explicit allowance is made of the finite lifetime of the isomeric nuclear state, which decays emitting a γ quantum with energy ω''. Analogously to Eq. (1), for a monochromatic incident photon ω', the expression for the cross-section of the process may be presented as follows:

$$\sigma_\gamma^{(4b)}(\omega') = D^{(a)}(\omega')\,\frac{\Gamma^{(\mathrm{NEET};4b)}/2\pi}{(\omega' - \omega_{8p-7s})^2 + (\Gamma_{8p}^{(a)}/2)^2}\,, \tag{11}$$

Table 1
Resonance transition energies ω_0, internal conversion coefficients α_d, and radiative widths for the reverse M1 transitions

Transition	Atom	ω_0, eV	α_d(M1), eV	$\Gamma_\gamma^{(a)}$, eV
$7s \to 8s$	neutral	3.44	$1.66 \cdot 10^{10}$	$0.880 \cdot 10^{-14}$
	ionised once	6.16	$5.47 \cdot 10^{10}$	$0.584 \cdot 10^{-14}$
	ionised twice	8.81	$1.13 \cdot 10^{10}$	$0.408 \cdot 10^{-14}$
$7s \to 7s$	neutral	0.00	$1.53 \cdot 10^{11}$	$0.120 \cdot 10^{-11}$
	ionised once	"	$2.64 \cdot 10^{11}$	$0.120 \cdot 10^{-11}$
	ionised twice	"	$4.04 \cdot 10^{11}$	$0.120 \cdot 10^{-11}$
$7p_{1/2} \to 7p_{1/2}$	neutral	0.00	$5.16 \cdot 10^{9}$	$0.666 \cdot 10^{-13}$
	ionised once	"	$1.16 \cdot 10^{10}$	$0.665 \cdot 10^{-13}$
	ionised twice	"	$2.02 \cdot 10^{10}$	$0.665 \cdot 10^{-13}$
$7p_{3/2} \to 7p_{3/2}$	neutral	0.00	$1.18 \cdot 10^{8}$	$0.200 \cdot 10^{-11}$
	ionised once	"	$4.80 \cdot 10^{8}$	$0.200 \cdot 10^{-11}$
	ionised twice	"	$1.08 \cdot 10^{9}$	$0.200 \cdot 10^{-11}$
$7p_{1/2} \to 8p_{1/2}$	neutral	2.30	$7.87 \cdot 10^{8}$	$0.846 \cdot 10^{-16}$
	ionised once	4.66	$3.02 \cdot 10^{9}$	$0.121 \cdot 10^{-16}$
	ionised twice	7.07	$6.80 \cdot 10^{9}$	$0.164 \cdot 10^{-17}$
$7p_{3/2} \to 8p_{3/2}$	neutral	1.65	$2.62 \cdot 10^{7}$	$0.761 \cdot 10^{-15}$
	ionised once	3.90	$1.44 \cdot 10^{8}$	$0.147 \cdot 10^{-15}$
	ionised twice	6.27	$3.85 \cdot 10^{8}$	$0.364 \cdot 10^{-16}$
$7p_{1/2} \to 7p_{3/2}$	neutral	0.77	$1.77 \cdot 10^{7}$	$0.247 \cdot 10^{-12}$
	ionised once	1.03	$5.37 \cdot 10^{7}$	$0.254 \cdot 10^{-12}$
	ionised twice	1.22	$1.06 \cdot 10^{8}$	$0.255 \cdot 10^{-12}$
$7p_{1/2} \to 8p_{3/2}$	neutral	2.42	$3.93 \cdot 10^{6}$	$0.626 \cdot 10^{-14}$
	ionised once	4.93	$1.61 \cdot 10^{7}$	$0.356 \cdot 10^{-14}$
	ionised twice	7.49	$3.79 \cdot 10^{7}$	$0.268 \cdot 10^{-14}$
$7p_{3/2} \to 8p_{1/2}$	neutral	1.52	$2.71 \cdot 10^{6}$	$0.394 \cdot 10^{-14}$
	ionised once	3.63	$1.40 \cdot 10^{7}$	$0.212 \cdot 10^{-14}$
	ionised twice	5.85	$3.59 \cdot 10^{7}$	$0.187 \cdot 10^{-14}$

The coefficients and the widths are calculated for a transition energy of 3.5 eV (see text).

where $\Gamma^{(\mathrm{NEET;4b})}$ is the partial width of the atomic decay of the $8p$ state via the NEET channel:

$$\Gamma^{(\mathrm{NEET;4b})} = \int d\omega''\, \alpha_d \frac{\Gamma_\gamma^{(n)}}{2\pi} \frac{\Gamma^{(n)}/2\pi}{(\omega'' - \omega_n)^2 + (\Gamma^{(n)}/2)^2} \times \frac{\Gamma^{(a)}(7p \to 7s; \omega''')/2\pi}{(\omega''' - \omega_{7p\text{-}7s})^2 + (\Gamma_{7p}^{(a)}/2)^2}, \tag{12}$$

and $D^{(a)}(\omega; 7s \to 8p)$ in Eq. (13) is obtained from Eq. (6) by replacing the nuclear radiative width by the atomic one, taken for the transition energy ω:

$$D^{(a)}(\omega; 7s \to 8p) = \frac{\pi^2}{\omega^2} \Gamma_\gamma^{(a)}(8p \to 7s; \omega) \frac{2I_{8p} + 1}{2I_{7s} + 1}. \tag{13}$$

The energies of the photons are related by conservation of energy: $\omega' = \omega'' + \omega'''$.

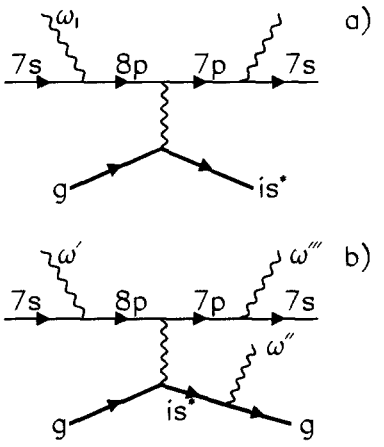

Fig. 4. "Symmetric" Feynman graph of the nuclear excitation through the electron shell (a), and the same process in finer detail (b).

Performing integration over ω'', taking into account Eq. (10), we arrive at the following expression for the cross-section of Fig. 4b:

$$\sigma_\gamma^{(4b)}(\omega') = D^{(a)}(\omega'; 7s \to 8p)\, \frac{\alpha_d(8p \to 7p; \omega_n)\Gamma_\gamma^{(n)}/2\pi}{(\omega' - \omega_{8p\text{-}7s})^2 + (\Gamma_{8p}^{(a)}/2)^2} \times \frac{\Gamma_\gamma^{(a)}(7p \to 7s; \omega''')/2\pi}{(\omega''' - \omega_{7p\text{-}7s})^2 + (\Gamma_{7p}^{(a)}/2)^2}\,. \tag{14}$$

The cross-section of Eq. (14) has two strong maxima corresponding to the two poles of the amplitude of Fig. 4b, when one of the two intermediate electron states turns out to be on the mass shell, i.e. when its energy coincides with the energy of the $8p$- (the first pole) or $7p$- (the second pole) state. The widths of both resonances are of the order of the corresponding atomic widths. Performing integration in Eq. (14) over the energy of the incident laser beam ω', we arrive at the expression for the cross-section of Fig. 4a. In the first case $\omega_l = \omega_{8p\text{-}7s}$, and we obtain

$$\sigma_\gamma^{(4a')}(\omega_l) = S(\omega_l)\, D^{(a)}(\omega_l)\, \frac{\alpha_d \Gamma_\gamma^{(n)}}{\Gamma^{(a)}(8p)}\, \frac{\Gamma^{(a)}(7p \to 7s; \omega_l - \omega_n)/2\pi}{(\omega_n - \omega_{8p\text{-}7p})^2 + (\Gamma_{7p}^{(a)}/2)^2} \equiv R\sigma_n(\omega_n)\,. \tag{15}$$

We thus factorised the expression into the nuclear cross-section and the acceleration factor R related to the electronic structure of the atom. Supposing the branching factor $\Gamma_\gamma^{(a)}(8p \to 7s; \omega_l)/\Gamma^{(a)}(8p)$ to be of the order of unity, with account of Eq. (6), the acceleration R factor may be essentially reproduced as follows:

$$R_4' = \frac{\alpha_d(8p \to 7p)\, \Gamma_\gamma^{(a)}(7p \to 7s; \omega_{8p\text{-}7s} - \omega_n)}{2\pi(\omega_{7p\text{-}8p} - \omega_n)^2}\,. \tag{16}$$

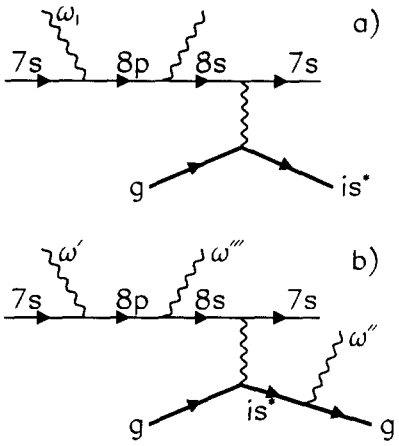

Fig. 5. Feynman graph of the process of nuclear excitation in electron transition NEET (a), and the same process in finer detail (b).

In the second case, the laser frequency is to be chosen as $\omega_l = \omega_n + \omega_{7p\text{-}7s}$, whose precise value is again not yet available. In this case, analogously to Eq. (14), we arrive at the following expression for the cross-section:

$$\sigma_\gamma^{(4a'')}(\omega_l) = \frac{S(\omega_l)\, D^{(a)}(\omega_l)\, \alpha_d \Gamma_\gamma^{(n)}/2\pi}{(\omega_l - \omega_{7s\text{-}8p})^2 + (\Gamma_{8p}^{(a)}/2)^2} \equiv R\sigma_n(\omega_n)\,, \tag{17}$$

and for the corresponding conversion factor R_4'':

$$R_4'' = \frac{\alpha_d(8p \to 7p)\, \Gamma_\gamma^{(a)}(8p \to 7s; \omega_{7p\text{-}7s} + \omega_n)}{2\pi(\omega_n - \omega_{8p\text{-}7p})^2} \left(\frac{\omega_l}{\omega_n}\right)^2. \tag{18}$$

The latter expression coincides with Eq. (9), as expected.

Finally, consider the graph of Fig. 5a. Making use of the more detailed graph Fig. 5b, we get an expression for the cross-section:

$$\sigma_\gamma^{(5b)}(\omega') = \int d\omega''\, D^{(a)}(\omega') \frac{\Gamma^{(a)}(8p \to 8s; \omega' - \omega_n)/2\pi}{(\omega' - \omega_{8p\text{-}7s})^2 + (\Gamma_{8p}^{(a)}/2)^2} \times \frac{\Gamma^{(\mathrm{NEET;5b})}/2\pi}{(\omega'' - \omega_{8s\text{-}7s})^2 + (\Gamma_{8s}^{(a)}/2)^2}\,, \tag{19}$$

where

$$\Gamma^{(\mathrm{NEET;5b})} = \alpha_d \frac{\Gamma^{(n)}}{2\pi} \frac{\Gamma^{(n)}/2\pi}{(\omega'' - \omega_n)^2 + (\Gamma^{(n)}/2)^2}\,. \tag{20}$$

Performing integration over ω'', we arrive at the following expression for the cross-section:

$$\sigma_\gamma^{(5b)}(\omega') = S(\omega')\, D^{(a)}(\omega')\, \frac{\Gamma^{(a)}((8p \to 7s; \omega' - \omega_n)/2\pi}{(\omega' - \omega_{8p-7s})^2 + \Gamma_{8p}^{(a)}/2)^2}$$
$$\times \frac{\alpha_d(8s \to 7s; \omega_n)\Gamma_\gamma^{(n)}/2\pi}{(\omega_n - \omega_{7s-8s})^2 + (\Gamma_{8s}^{(a)}/2)^2}\,. \tag{21}$$

And after integrating over the energy of the incident laser beam, we obtain

$$\sigma_\gamma^{(5a)}(\omega_l) = S(\omega_l)\, D^{(a)}(\omega_l; 7s \to 8p)\, \frac{\alpha_d \Gamma_\gamma^{(n)}/2\pi}{(\omega_n - \omega_{7s-8s})^2 + (\Gamma^{(a)}(8s)/2)^2}$$
$$\equiv R\sigma_n(\omega_l)\,. \tag{22}$$

The cross-section of Eq. (22) has a very transparent structure. It can be represented as follows:

$$\sigma_\gamma^{(5a)}(\omega_l) = \sigma_\gamma^{(a)}(7s \to 8p)\, P_{\mathrm{NEET}}(8p \to 7s)\,, \tag{23}$$

where $\sigma_\gamma^{(a)}(7s \to 8p)$ is the cross-section of the atom photoexcitation $7s \to 8p$, and $P_{\mathrm{NEET}}(8p \to 7s)$ is the NEET probability of the subsequent electron transition:

$$P_{\mathrm{NEET}}(8p \to 7s) = \frac{\alpha_d \Gamma_\gamma^{(n)}/2\pi}{(\omega_n - \omega_{7s-8s})^2 + (\Gamma^{(a)}(8s)/2)^2}\,. \tag{24}$$

As expected, the latter expression coincides with that obtained in Ref. [5] in another way.

The numerical value and the nature of the accelerating factor R immediately follows from Eq. (23). Our gain is as large as the ratio of the atomic-to-nuclear photoabsorption cross-sections, times the NEET probability of the subsequent electron transition:

$$R_5 = \frac{\sigma_a}{\sigma_n} P_{\mathrm{NEET}} = \left(\frac{\omega_l}{\omega_n}\right)^2 \frac{\Gamma_\gamma^{(a)}}{\Gamma_\gamma^{(n)}}\, P_{\mathrm{NEET}}\,. \tag{25}$$

Substituting Eq. (24) into (25), we obtain the factor R_5 in the following form:

$$R_5 = \frac{\alpha_d(7s\text{–}8s)\, \Gamma_\gamma^{(a)}(8p\text{–}7s; \omega_{8p-7s})}{2\pi\Delta^2} \left(\frac{\omega_l}{\omega_n}\right)^2 \frac{\Gamma_\gamma^{(a)}(8p\text{–}8s; \omega_l - \omega_n)}{\Gamma_{8p}^{(\mathrm{tot})}}\,. \tag{26}$$

The latter expression can be further simplified by omitting branching ratios and other factors of the order of unity:

$$R_5 = \frac{\alpha_d(7s\text{–}8s)\, \Gamma_\gamma^{(a)}(8p\text{–}7s; \omega_l)}{2\pi\Delta^2}\,. \tag{27}$$

3. Results of the calculation

Results of the calculation for the ICC, radiative widths are summarised in Tables 1 and 2. The calculations have been made within the framework of the self-consistent

Table 2
Resonance transition energies ω_0, and radiative widths for the E1 transitions as calculated for a transition energy of 3.5 eV (see text)

Transition	Atom	ω_0, eV	$\Gamma_\gamma^{(a)}$, eV
$7p_{1/2} \rightarrow 7s$	neutral	1.64	$0.104 \cdot 10^{-6}$
	ionised once	2.49	$0.821 \cdot 10^{-7}$
	ionised twice	3.22	$0.692 \cdot 10^{-7}$
$7p_{3/2} \rightarrow 7s$	neutral	2.41	$0.960 \cdot 10^{-7}$
	ionised once	3.52	$0.779 \cdot 10^{-7}$
	ionised twice	7.67	$0.657 \cdot 10^{-7}$
$8p_{1/2} \rightarrow 7s$	neutral	3.94	$0.180 \cdot 10^{-9}$
	ionised once	7.16	$0.1 \cdot 10^{-10}$
	ionised twice	10.30	$0.246 \cdot 10^{-10}$
$8p_{3/2} \rightarrow 7s$	neutral	4.06	$0.296 \cdot 10^{-8}$
	ionised once	7.43	$0.952 \cdot 10^{-9}$
	ionised twice	10.72	$0.429 \cdot 10^{-9}$
$8s \rightarrow 7p_{1/2}$	neutral	1.80	$0.110 \cdot 10^{-6}$
	ionised once	3.67	$0.672 \cdot 10^{-7}$
	ionised twice	5.59	$0.488 \cdot 10^{-7}$
$8s \rightarrow 7p_{3/2}$	neutral	1.03	$0.110 \cdot 10^{-6}$
	ionised once	2.63	$0.270 \cdot 10^{-6}$
	ionised twice	4.37	$0.565 \cdot 10^{-6}$

Fock–Dirac method by use of the package of the computer codes [23,24]. For the electric dipole transitions, the radiative widths are calculated in the length gauge, because only this gauge provides a correct long-wavelength limit, when the widths are proportional to the transition energy ω^3, and can be expressed in terms of the nonrelativistic matrix element of the transition operator $r^L Y_{LM}$. In the other gauges, the widths are not proportional to ω^3 [25]. In Table 1, the ICC, radiative widths and the transition energies are presented for the M1 transitions. The magnetic transitions are gauge invariant. For the present purposes, we only need the radiative M1 widths for the $7s \rightarrow 8s$ transitions. In Table 2, the radiative dipole transition rates, with the resonance energies are listed for neutral atoms and for one- and two-fold ions of Th. The ICC and $\Gamma_\gamma^{(a)}$ are calculated for a transition energy of 3.5 eV. For other energies, $\Gamma_\gamma^{(a)}$ may be obtained by scaling, supposing proportionality to ω^3 [5], and $\alpha_d \sim \omega^{-3}$ [22].

Let us consider step by step the effectiveness of the diagrams presented in Figs. 2 to 5.

Fig. 2a. In this case, the laser frequency must be precisely equal to the nuclear frequency: $\omega_l = \omega_n$. By means of the values presented in Table 1, we find for the neutral atom of Th: $\Delta = 0.06$ eV, $R^{(2a)} = 0.0065$ for the chain of transitions $7s \rightarrow 8s \rightarrow 7s$, and 0.0024 for the chain $7s \rightarrow 7s \rightarrow 7s$. Or, summing coherently the amplitudes of the process, we arrive at the total magnitude of the effect $R^{(2a)} = 0.017$. In this simple mechanism, the electron shell happens not to be an effective resonator!

Figs. 3a and 3c. For the graph of Fig. 3a, the enhancement factor R can be calculated

Table 3
Resonant laser frequency ω_l, resonance atomic frequency ω_0, and enhancement factor R for the mechanism presented by Fig. 3

Feynman graph	Transition	ω_0, eV	ω_l, eV	R
Fig. 3a	$7s$–$8p_{1/2}$–$7p_{1/2}$	3.94	5.14	0.099
	$7s$–$7p_{1/2}$–$7p_{1/2}$	1.64	5.14	44.2
	$7s$–$7p_{3/2}$–$7p_{1/2}$	2.41	5.14	0.23
	$7s$–$8p_{3/2}$–$7p_{1/2}$	4.06	5.14	0.010
	$7s$–$7p_{1/2}$–$7p_{3/2}$	1.64	5.91	0.16
	$7s$–$7p_{3/2}$–$7p_{3/2}$	2.41	5.91	1.42
	$7s$–$8p_{3/2}$–$7p_{3/2}$	4.06	5.91	0.035
	$7s$–$8p_{1/2}$–$7p_{3/2}$	3.94	5.91	$1.93 \cdot 10^{-4}$
Fig. 3c	$7s$–$7s$–$7p_{1/2}$	–	5.14	654
	$7s$–$7s$–$7p_{3/2}$	–	5.91	918

Table 4
Resonant laser frequency ω_l, resonance atomic frequency ω_0, and enhancement factor R for the mechanism presented by Fig. 4

Transition	ω_l, eV	ω_0, eV	R
$7s$–$8p_{1/2}$–$7p_{1/2}$–$7s$	3.94	1.64	$1.79 \cdot 10^{-2}$
$7s$–$8p_{3/2}$–$7p_{3/2}$–$7s$	4.06	2.41	$2.39 \cdot 10^{-4}$

by means of Eq. (9). The laser frequency is the sum of the nuclear frequency plus excitation energy of the atom in the final state: $\omega_l = \omega_n + \omega_a$. The results are presented in Table 3. Note that the discrete conversion coefficients α_d for the transitions with different values of the total electron angular momentum j turn out to be less than those with the same values of j by an order of magnitude. As a result, contributions from these transitions are much smaller.

As one can see from Table 3, the dominant contribution comes from the $7p_{1/2}$ level as intermediate and final states of the excited atom. Indeed, the enhancement factor is greater than unity now: $R \approx 40$, as was expected, due to the allowed electric dipole vertex in the interaction of the atom with the electromagnetic field of a laser.

The results for the graph of Fig. 3c are presented in the same table. As it was expected, the R factor is much greater in this case.

Fig. 4a. Here we only have to calculate R'_4 as given by Eq. (16). We need not calculate R''_4 given by Eq. (18), as the corresponding contribution becomes equal to the one which is given by Fig. 3a. For R'_{4a}, only two possibilities can be conceived for a neutral atom: $7s$–$8p_{3/2}$–$7p_{3/2}$–$7s$ and $7s$–$8p_{1/2}$–$7p_{1/2}$–$7s$. Here, the intermediate $8p$ state cannot be replaced by a $7p$ one, because both $7p_{1/2}$ and $7p_{3/2}$ states have energies below 3.5 eV, the supposed energy of the isomeric state. The results are presented in Table 4. In this case, the laser frequency $\omega_l = \omega_{7s\text{–}8p}$ is equal to the resonance frequency of photoexcitation of the atom to the $8p$ state. The frequency of the scattered photon $\omega''' = \omega_l - \omega_n$, and the atomic resonance frequency $\omega_0 \equiv \omega'''$ are both equal to the

excitation energy of the $7p$ state of the atom ω_{7s-7p} in the second intermediate state.

Fig. 5a. In this case, as in the previous one, the laser frequency $\omega_l = \omega_{7s-8p}$ is equal to the resonance frequency of photoexcitation of the atom to the $8p$ state. The frequency of the scattered photon $\omega''' = \omega_l - \omega_n$ also remains the same, only the order of emission of a photon with energy ω''' and nuclear excitation is inverted. A consequence, however, is that for the graph of Fig. 5, the nuclear excitation occurs in the $7s$–$8s$ electronic transition, for which transition the ICC α_d are maximal. The latter circumstance is due to the fact that the wavefunction at the origin is proportional to r^l, and, therefore, is maximal for the s states. (Erroneously, in papers [26] the conversion in the $6d$ state has been taken into account instead of the $7s$ shell. This error led to an underestimate of the effect considered by three orders of magnitude. The latter question is considered in finer detail in Ref. [7]).

Let us consider two chains of electron transitions, $7s$–$8p\frac{1}{2}$–$8s$–$7s$ and $7s$–$8p\frac{3}{2}$–$8s$–$7s$. From Table 2, we find the corresponding laser frequencies: $\omega_l = 3.94$ and 4.06 eV, and the radiative widths corrected for the actual transition energies [3]: $\Gamma_\gamma^{(a)}(8p \rightarrow 7s; \omega_l) = 2.57 \cdot 10^{-10}$ and $4.62 \cdot 10^{-9}$ eV, respectively.

Substituting these values into Eq. (27), with the value of $\alpha_d = 1.66 \cdot 10^{10}$ eV from Table 1, we obtain an estimate $\Delta = 0.06$ eV, resulting in the R_5 values of $R_5 = 3.39 \cdot 10^3$ and $R_5 = 132$ for the chains of transitions through the $8p\frac{3}{2}$ and $8p\frac{1}{2}$ states, respectively. It is a pleasure for the authors to note that this mechanism first proposed in Ref. [3] turns out to have the absolutely largest cross-section, in comparison with others considered previously, thus passing a very critical test. Moreover, the undoubted merit of the mechanism is that it needs no knowledge of the energy of the nuclear isomeric state. Conversely, the latter can be obtained from experiment, along with the electromagnetic strength of the transition between the ground state and the isomeric nuclear state. It is remarkable that a pumping cycle through the $8p\frac{3}{2}$ state turns out more preferable on the basis of the present, more general consideration. Within the scope of paper [3], the other cycle through the $8p\frac{1}{2}$ state looked more efficient, although the latter cycle remains sufficiently effective, and retains all the other merits of the mechanism of Fig. 5.

For the one- and two-fold ions, the most important change is that of the transition energies, and the related increase of the laser frequency, as follows from Tables 1 and 2. Radiative widths and ICC do not change so drastically, within tens of a percent, which seems not to be important at the present stage of experimental investigation.

4. Shake excitation in heavy ions

A Feynman graph of the process of ionisation of the electron shell of an incoming atom in collision with the target atom is presented in Fig. 6a. The amplitude of the process can be expressed as

$$F_{\mathrm{sh}} = \sum_n \frac{F_{\mathrm{c}}^{(n)} F_{\mathrm{ion}}^{(n)}}{E_n + E_n^{(a)} - E_{1s}^{(a)}} \,. \tag{28}$$

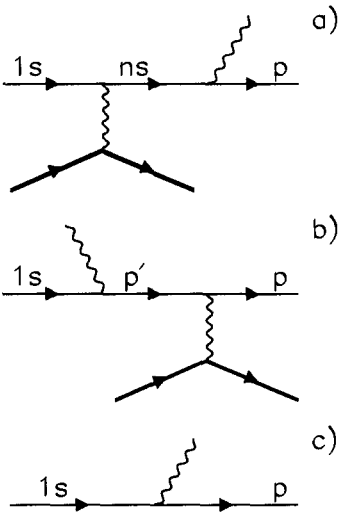

Fig. 6. Feynman graph of the nuclear excitation due to disappearance of the electrons from the shells through shake (a), by the Coulomb field of the ionisation outgoing electron (b), and ionisation without nuclear excitation (c). p, p' denote the four-momenta of the final and intermediate electrons, respectively.

Here $F_c^{(n)}$ is an elementary amplitude of the virtual process of reverse conversion in the incoming atom. In the process, an electron is "promoted" from the $1s$ to an excited state n. The energy is, however, transferred from the electron to the nucleus, so that the "converted" electron goes down below the mass shell (cf. Fig. 3c). Then the electron is knocked out in collision with the target nucleus, which causes the ionisation. $F_{\rm ion}^{(n)}$ is just the ionisation amplitude of the atom from the nth state by the external Coulomb field of the target nucleus. The conversion probability is known to be proportional to $|\psi_n(0)|^2\ 1/n^3$ (Ref. [22] and Eq. (32) below), so that the series (28) converges rapidly. In fact, account of the single $1s$ state in the spectral representation of the electron propagator in series (28) is sufficient for the present purposes. As a result, the amplitude of the process acquires the following form:

$$F_{\rm sh} = \frac{F_c^{(1s)} F_{\rm ion}^{(1s)}}{E_n}\,. \tag{29}$$

This should not be confused with the amplitude of Fig. 6b. In the latter case, the fast ionisation electron excites the nucleus by its Coulomb field. For the M1 nuclear excitation, the probability of the latter process is much less.

Expressing the conversion width in terms of the ICC and the radiative nuclear width, we obtain from Eq. (27) the following expression:

$$\Gamma_{\rm sh} = \frac{\Gamma_c \Gamma_{\rm ion}/2\pi}{E_n^2} \equiv \frac{\alpha_d \Gamma_\gamma^{(n)} \Gamma_{\rm ion}}{2\pi E_n^2}\,. \tag{30}$$

The shake-on probability is obtained from Eq. (28) by dividing by the ionisation probability per unit time $\Gamma_{\rm ion}$, the Feynman graph of which is presented in Fig. 6b. As a result, the ionisation probability is cancelled in the ratio

$$P_{\text{shake}} = \frac{\alpha_d \Gamma_\gamma^{(n)}}{2\pi E_n^2} \,. \tag{31}$$

The ICC for the $1s \to 1s$ transition can be obtained with the relativistic Coulomb wavefunctions, as electron screening is negligible for the $1s$ state, by means of the following formula (see e.g. Ref. [22]):

$$\alpha_d(\mathrm{M1}; 1s \to ns) = \frac{\alpha\pi N_K}{6m^2\omega^3} \left|\psi_{1s}(0)\, \psi_{ns}(0)\right|^2 , \tag{32}$$

with the population number of the initial $1s$ shell N_K, and the radial wave function $\psi(r)$. The latter expression is proportional to the electron density at the nucleus in the initial and final states, which are proportional to $|\psi(0)|^2 \sim n^{-3}$. Therefore, the other states can be neglected, apart from the $1s$ states for both the initial and final electrons. By straightforward calculation, one arrives at the following expression:

$$\alpha_d(\mathrm{M1}; 1s \to 1s) = \frac{2}{3} \frac{\alpha\pi}{\omega^3} \frac{\eta^4(1-\gamma^2)}{\gamma^2(2\gamma-1)^2} \,, \tag{33}$$

which results in the numerical value $\alpha_d(\mathrm{M1}; 1s \to 1s) = 1.33 \cdot 10^{13}$ MeV. This leads to the excitation probability of the isomeric nuclear state of $6.72{\cdot}10^{-4}$ per removed $1s$ electron. We note that if both $1s$ electrons are removed consecutively, there is a chance for the nucleus to be excited at every step. Therefore, the probability found above doubles, achieving $1.34{\cdot}10^{-3}$ per atom.

We note that for a muonic atom, $|\psi(0)|^2 \sim m_\mu^3$. On the other hand, the magnetic moment of the muon is less than the electron one by m_μ/m_e. Therefore, in this case one should expect the shake-on probability to be greater by $(m_\mu/m_e)^4$, which directly follows Eq. (33). There are two strong effects: static and dynamic ones, arising in muonic atoms due to the finite nuclear size, which reduce the M1 ICC by about three orders of magnitude for the atoms with atomic numbers $Z \approx 90$ [29]. Nevertheless, we still arrive at an estimate for the excitation probability in disintegration of the muon in the orbit, which turns out to be of the order of unity. Such a high probability is due to the uniquely small energy of the isomer, as the probability is inversely proportional to the energy cubed. Otherwise, if the transition nuclear energy is about 10 keV or more, as is usually the case, one immediately finds that the excitation probability reduces to a value of the order of 10^{-6} only. Qualitatively, the latter value is close to the calculation [27] of the excitation probabilities of the monopole E0 nuclear states in the muon decay in the orbit, as it should be expected on physical grounds.

5. About experimental proposals for discovering NEET in spin–flip transitions in H-like ions $^{229}Th^{89+}$

The effect of the excitation of the 3.5eV isomer in 89-fold hydrogen-like $^{229}Th^{89+}$ ions may be discovered by measuring transition rates between hyperfine structure components. It was noted in Ref. [10] that due to an extremely low energy, the hyperfine interaction

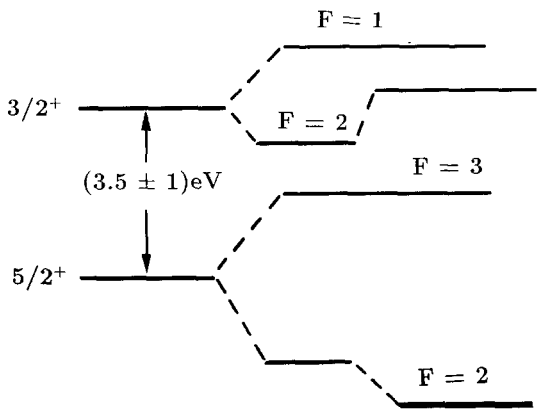

Fig. 7. Scheme of the hyperfine components corresponding to the doublet nuclear states of the H-like ion of ^{229}Th.

arising in the H-like ions of ^{229}Th can mix nuclear states of the same parity, but differing by one unit of spin. Such mixing leads to a drastic effect of acceleration of the nuclear deexcitation from the isomeric state [6]. This occurs via spin–flip of the orbital electron, just as transitions between normal components of the hyperfine structure. To better realise the effect, one can imagine a neutral atom of ^{229m}Th with an excited nucleus. Its lifetime is hours, as mentioned before. If, however, all the electrons are stripped but one, or merely a hole is produced in the K shell, the nucleus gets deexcited promptly! This mechanism of acceleration may be compared to acceleration of interband transitions arising due to Coriolis mixing.

A relevant experiment could be conceived at GSI, in Darmstadt, where hyperfine structure of ^{209}Bi has been recently measured [28]. Efforts should be made to detect the energies and lifetimes of the transitions. Then the four values: $B(\mathrm{M1})$, E_{isom}, magnetic moments μ_1 and μ_2 in the ground and excited states, are unambiguously determined by the experimentally observable lifetime of any of the transitions involving the $F = 2$ component, and three energies of the excited hyperfine components (with respect to the ground level with $F = 2$). The theory, and some possible ways of realising the experiment are described in detail in Ref. [6].

6. Conclusion

The main results of the present consideration can be formulated as follows:

(1) In certain cases of resonance, the electron shell is really able to work as a very efficient resonator which significantly enhances the interaction of the nucleus with an externally applied laser field.

(2) It may be concluded that most feasible for experimental study is the mechanism based on the NEET process in the $7s$–$8s$ electronic transition (Fig. 5a). In this case, the enhancing factor R reaches four orders of magnitude.

(3) A new effective process for the excitation of the isomeric level has been found. This is shake up arising in muon decay in the orbit. The probability of excitation of the isomer in this case turns out to be of the order of unity. This effect may become a most effective tool for pumping the 3.5-eV isomer in ^{229}Th. A corresponding experimental study can be performed in the meson factories LAMF, TRIUMPH, PSI Villigen, Pakhra in Moscow.

(4) The hyperfine interaction in 89-fold hydrogen-like $^{229}Th^{89+}$ ions causes drastic acceleration of the nuclear deexcitation from the isomeric state. This effect can be used for experimental discovery of isomer excitation in the NEET process via spin–flip transitions. Additionally, full spectroscopic information about the ground and isomer levels will be obtained, and a new effect of the nuclear spin mixing discovered in such an experiment.

Acknowledgements

The authors are grateful to M.R. Seizew and J. da Providencia for their attention to the paper, and to A. Pastor for valuable discussions. This work has been supported by the PRAXIS-XXI Program, Defence Special Weapons Agency (USA) under contract No. DSWA01-98-C-0040, and by Grant Nos. 96-02-18039-a and 99-02-17550 of the Russian Fund for Basic Research.

References

[1] C.W. Reich and R.G. Helmer, Phys. Rev. Lett. 64 (1990) 271.
[2] R.G. Helmer and C.W. Reich, Phys. Rev. C 49 (1994) 1845.
[3] F.F. Karpeshin et al., Phys. Lett. B 282 (1992) 267.
[4] F.F. Karpeshin et al., Invited talk presented at the 2nd Int. Conf. on Nucl. Shapes and Nucl. Structure at Low Excitation Energies, Antibes (France) 20–25 June, 1994.
[5] F.F. Karpeshin, I.M. Band, M.B. Trzhaskovskaya and M.A. Listengarten, Phys. Lett. B 372 (1996) 1
[6] F.F. Karpeshin, S. Wycech, I.M. Band, M.B. Trzhaskovskaya, M. Pfützner and J. Żylicz, Phys. Rev. C 57 (1998) 3085.
[7] F.F. Karpeshin, I.M. Band, M.B. Trzhaskovskaya and A. Pastor, Phys. Rev. Lett., in press.
[8] P. Kálmán and T. Keszthelyi, Phys. Rev. A 47 (1993) 1320; C 49 (1994) 324.
[9] E.V. Tkalya. Nucl. Phys. A 539 (1992) 209.
[10] S. Wycech and J. Żylicz, Acta Phys. Pol. B 24 (1993) 637 and references quoted therein.
[11] G.M. Irwin and K.H. Kim, Phys. Rev. Lett. 79 (1997) 990.
[12] D.S. Richardson et al., Phys. Rev. Lett. 80 (1998) 3206.
[13] S.B. Utter et al., Phys. Rev. Lett., in press.
[14] R.W. Shaw et al., Phys. Rev. Lett., in press
[15] J.A. Wheeler, Phys. Rev. 73 (1948) 1252;
D.F. Zaretsky and V.M. Novikov, Nucl. Phys. 14 (1959) 540; 28 (1961) 177;
E. Teller and M.S. Weiss, Trans. NY Acad. Sci. 40 (1980) 222;
F.F. Karpeshin and V.O. Nesterenko, J. Phys. G 17 (1991) 705.
[16] L.D. Landau and E.M. Livshitz, Quantum Mechanics, Nonrelativistic Theory (Pergamon, London, 1958).
[17] I.S. Batkin, Sov. J. Nucl. Phys. 29 (1979) 464.
[18] D.F. Zaretsky and V.M. Lomonosov, Yad. Fiz. 41 (1985) 655 [Sov. J. Nucl. Phys. 41 (1985) 417].
[19] F.F. Karpeshin et al., JETP 97 (1990) 401; Can. J. Phys. 70 (1992) 623.

[20] P. Kálmán, Phys. Rev. A 47 (1991) 2603.
[21] M. Morita, Prog. Theor. Phys. 49 (1973) 1574.
[22] F.F. Karpeshin, M.R. Harston, F. Attallah, J.F. Chemin et al., Phys. Rev. C, in press.
[23] I.M. Band and M.B. Trzhaskovskaya, At. Data Nucl. Data Tables 55 (1993) 43.
[24] I.M. Band, M.A. Listengarten, M.B. Trzhaskovskaya and V.I. Fomichev, Program Complex RAINE, Leningrad, PNPI Vols. 289 (1976), 298–300 (1977) and 1479 (1989).
[25] I.P. Grant, J. Phys. B 12 (1974) 1458.
[26] V.F. Strizhov and E.V. Tkalya, Zh. Exp. Teor. Fiz. 99 (1991) 697;
E.V. Tkalya, Lett. to Zh. Exp. Teor. Fiz. 55 (1992) 216.
[27] I.S. Batkin, Sov. J. Nucl. Phys. 24 1976 235; 28 (1976) 745; 29 (1979) 749.
[28] M. Finkbeiner, B. Fricke and T. Kühl, Phys. Lett. A 176 (1993) 113.
[29] F.F. Karpeshin, M.A. Listengarten, I.M. Band and L.A. Sliv, Izv. Akad. Nauk SSSR, ser. fiz. 40 (1976) 1164 [Bull. Acad. Sci. USSR, Phys. Ser. (USA) 40 (1976)].